Investigation on Transversal Anisotropy of an Aluminum Sheet for Crash Applications

F. Andrade[1], M. Feucht[2], C. Wilking[1], D. Koch[3]
[1]DYNAmore GmbH, Stuttgart, Germany
[2]Mercedes-Benz AG, Sindelfingen, Germany
[3]DYNAmore GmbH, Material Competence Center (MCC), Leinfelden-Echterdingen, Germany

Abstract

*In this paper, we concentrate our efforts on the simulation of an aluminum sheet material used in the automotive industry. A series of experiments using samples with different geometries is performed in order to characterize the material under different stress states. Plasticity is considered using a von Mises based and a Barlat based material model (respectively, *MAT_024 and *MAT_036 in LS-DYNA®). For the Barlat-based model, it is assumed that the R-values are the same for all material directions, a suitable assumption for 6000 aluminum sheets. This means that anisotropy is only present through the thickness and not in the plane of the material. In turn, this allows a more straightforward usage of *MAT_036 in complex parts for which no mapping of material directions have to be undertaken because the thickness direction for shell elements is known* a priori*. Comparison with experimental data (including strain fields measured with DIC) shows that this strategy leads to a somewhat better description of the material deformation observed in physical tests when compared to the predictions of the isotropic model *MAT_024. Finally, the GISSMO failure/damage model is adopted for the failure description in LS-DYNA. It is shown that the numerical results agree very well with the experiments and not only the global force-displacement curve but also the local strain fields.*

Introduction

In this paper, we focus on the accurate material modeling of aluminum sheets aiming at car crash simulations. Typically, an isotropic model like *MAT_024 in LS-DYNA is used to describe material deformation in crash simulations. Several reasons contribute to that choice, including numerical robustness and efficiency. Furthermore, an isotropic model does not require the information about preferred material directions like anisotropic material models do. However, most materials do behave in an anisotropic fashion, which lead to a certain loss of accuracy in the material modeling.

In this contribution, we investigate the use of a simplified anisotropic approach through *MAT_036. As a matter of fact, aluminum sheets of the 6000 family often exhibit similar R values in the 0°, 45° and 90° directions. For such cases, it is possible to assume an R value which is the same for all directions but not equal to 1.0 (i.e., R00=R45=R90≠1.0). By doing this, the need of knowing the material directions after a manufacturing step like typical metal forming vanishes. Also, the anisotropy described by such approach is merely of transversal nature which can be understood as a through-thickness anisotropic behavior. This simplification highly facilitates its employment in car crash simulations whose formed parts are typically too complex to effectively map the material directions in an efficient and straightforward manner.

The gain of such approach would be the more accurate description of sheet thinning (or thickening) when compared to the typical approach with *MAT_024 (which basically corresponds to the case when the R-value is equal to 1.0). In turn, the more accurate description of plastic deformation could contribute to an overall better failure prediction. Therefore, we carry out a study in this paper in order to investigate the effectiveness of using

*MAT_036 with R00=R45=R90≠1.0 as well as the numerical efficiency when compared to the typical approach with *MAT_024.

In the following sections, we will address the subject by first reporting the results of the physical tests performed for the material used in this study. Subsequently, we will shortly review the theory behind *MAT_024 and *MAT_036, followed by the parameter identification for these models based on the experimental results available. Finally, a performance study comparing the efficiency of both models will be presented, followed by some conclusions.

Experimental Testing

Effective material testing is necessary in order to characterize the material deformation and failure behavior. During the present study, several aluminum alloys in T4 sheet condition were physically tested at the Material Competence Center (MCC) located in Leinfelden-Echterdingen, in Germany.

Aiming at a car crash application, two tensile, a notched, an equibiaxial, a plate bending and two shear-tensile tests were performed using a universal testing machine and a DIC system to optically measure the strain fields (see Fig. 1). The tensile tests were performed in 0°, 45° and 90° directions with respect to the rolling direction of the aluminum sheet with the goal of identifying the anisotropic behavior of the material (at least under tension). In particular, the R-value for the different directions is directly obtained from the strain fields optically measured during the experiment. The R-value, defined as $R = \dot{\varepsilon}_{22}/\dot{\varepsilon}_{33}$, is considered here constant throughout deformation up to the necking point in a tensile test (i.e., $R \approx \varepsilon_{22}/\varepsilon_{33}$).

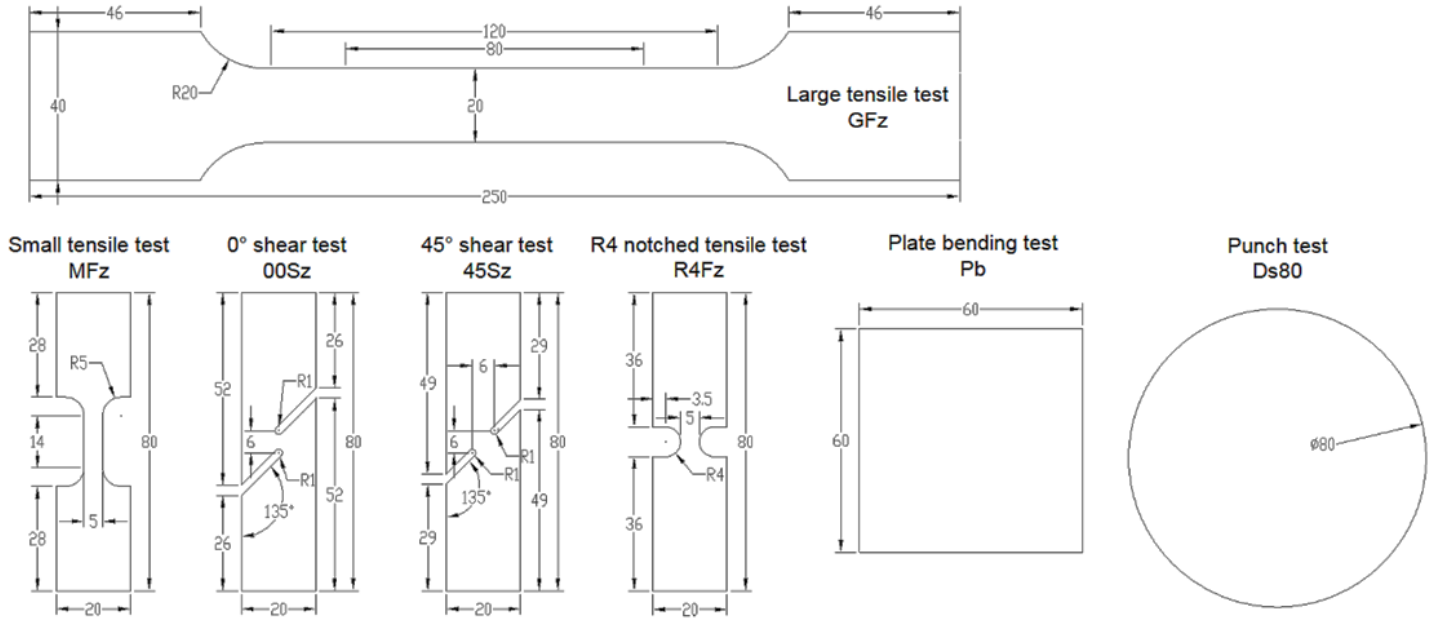

Figure 1. Overview of the samples used in the experimental characterization

In the present contribution, we will use the experimental data of one of the alloys which corresponds to a high strength aluminum sheet to be used in structural relevant components. The material chosen exhibits very similar R-values in the three directions whose average value is close to R=0.6 (here assumed constant throughout plastic deformation). Therefore, we will use this value in the subsequent analysis.

For the sake of brevity, we will restrict ourselves to the use of the small tensile, the notched and the shear 0° test in this document. For the goal of using *MAT_036 instead of *MAT_024, these three tests will be sufficient to demonstrate the effect of such choice and to draw the necessary conclusions. Nevertheless, in the final material card, all experiments performed where used in the parameter identification process.

Material Modeling

The yield function used in *MAT_024 is given by

$$\Phi(\boldsymbol{\sigma}) = \sigma_{eq} - \sigma_y = 0 \tag{1}$$

where $\sigma_{eq} = \sqrt{J_2(\boldsymbol{s})}$ is the von Mises equivalent stress. This model is isotropic and no material directions are considered in the formulation.

The model implemented in *MAT_036 (or *MAT_3-PARAMETER_BARLAT) was proposed by Barlat and Lian in 1989 [1], see LS-DYNA Keyword User's Manual Vol. 2 [2]. The yield function is defined as

$$\Phi(\boldsymbol{\sigma}) = \sigma_{eff} - \sigma_y = 0 \tag{2}$$

where

$$\sigma_{\text{eff}} = \left[\frac{1}{2}\left(a|K_1 + K_2|^m + a|K_1 - K_2|^m + c\,|2K_2|^m\right)\right]^{1/m} \tag{3}$$

$$K = \frac{\sigma_x + h\,\sigma_y}{2}, \quad K_2 = \sqrt{\left(\frac{\sigma_x - h\,\sigma_y}{2}\right)^2 + p^2\sigma_{xy}^2} \tag{4}$$

As can be seen in Equations (2) and (3), this model does not explicitly have the R-values in the formulation of the yield function. Nevertheless, Barlat and Lian have shown that it is possible to correlate the material parameters a, c, h and p to the R values through

$$a = 2 - 2\sqrt{\left(\frac{R_0}{1+R_0}\right)\left(\frac{R_{90}}{1+R_{90}}\right)}, \qquad c = 2 - a, \qquad h = \sqrt{\left(\frac{R_0}{1+R_0}\right)\left(\frac{1+R_{90}}{R_{90}}\right)} \tag{5}$$

The parameter "p" can be iteratively determined from

$$R_{45} = \frac{2m\sigma_y^m}{\left(\frac{\partial\Phi}{\partial x} + \frac{\partial\Phi}{\partial y}\right)\sigma_{45}} \tag{6}$$

Another important feature of the material model proposed by Barlat and Lian is that its yield function (and therefore its yield locus) is not necessarily quadratic. In fact, the order of the yield locus can be defined through the parameter "m" which is an exponent affecting the effective stress in Eq. (3). If m=2 and R00=R45=R90=1.0, *MAT_024 can be reproduced.

For transversal anisotropy where the three R-values are the same, the yield locus in the σ_1-σ_2 space is isotropic, but not necessarily equal to the yield locus obtained for *MAT_024. In fact, the exponent "m" also has an effect on the shape of yield locus which is no longer quadratic if m≠2. Barlat and Lian recommended m=8 for aluminum alloys.

Parameter Identification: Plasticity and Failure

In this Section, we firstly identify the parameters necessary for the elastoplastic description of the material. In both cases of *MAT_024 and *MAT_036 a hardening curve is necessary. In the case of *MAT_036, the exponent "m" and the R-values are further needed. As alluded in the Section on the experimental testing procedure, the present alloy exhibits an average R-value close to R=0.6 in all directions. Therefore, apart from the hardening curve, the only parameter left to identify in *MAT_036 is the exponent "m".

Figure 3 shows the simulation results obtained with *MAT_024, *MAT_036 with m=2 and *MAT_036 with m=8 when using the same hardening curve. In the present example, the hardening curve used has been identified as the one which best describes the experimental data for an exponent m=8 (which is the recommended value for aluminum by Barlat and Lian in their paper). As can be seen in Figure 3, *MAT_024 and *MAT_036 with m=2 do not quite reproduce the engineering stress strain curve measured in the tensile test.

Furthermore, Figure 4 shows the strain field optically measured in the experiment and the strain fields obtained in the different simulations. Observing Figure 4, we can conclude that *MAT_024 has a slight disagreement with the experiment meanwhile *MAT_036 with m=2 and with m=8 come closer to the strain values measured in the physical test.

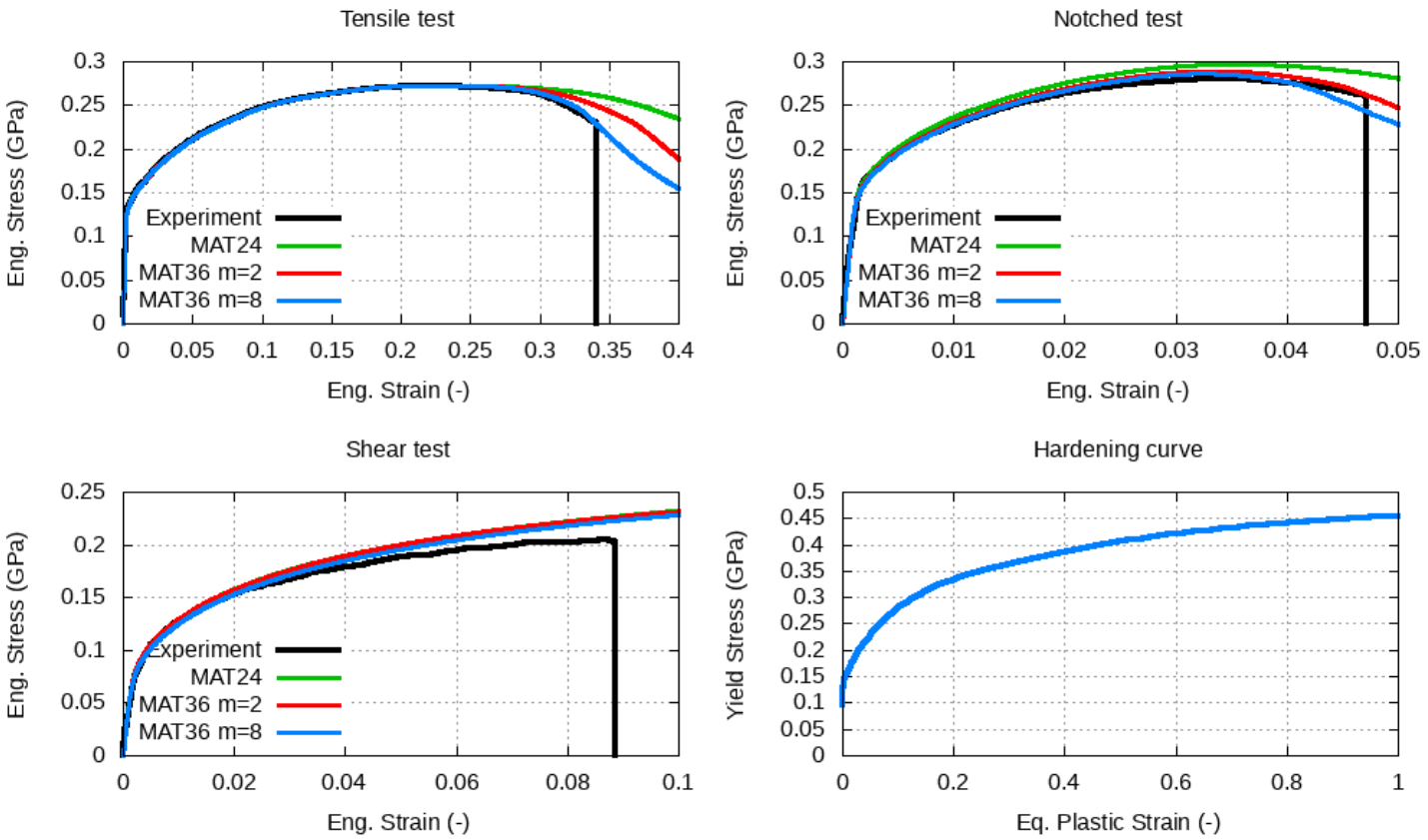

Figure 3. Overview of the simulation results with the same hardening curves for all three cases (*MAT_024, *MAT_036 with m=2, *MAT_036 with m=8).

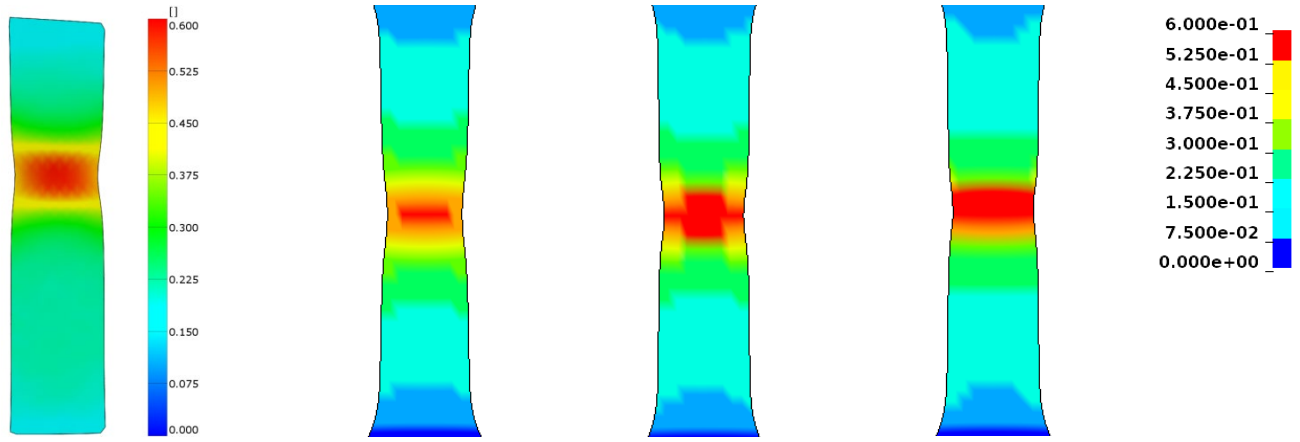

(a) Experiment (b) *MAT_024 (c) *MAT_36 m=2 (d) *MAT_36 m=8

Figure 4. Contours of major strain. The same hardening curve was used in the simulation in (b), (c) and (d).

At this point, one might ask what would be necessary in order to obtain a better description with *MAT_024 or even with *MAT_036 with m=2. By varying the hardening curve in these material models one can vary the response regarding material description. In the case of *MAT_024, which basically can be understood as the case when one has R=1.0, a hardening curve which is much flatter than the one initially identified for *MAT_036 with m=8 is necessary in order to reproduce the thinning of the tensile test. In the case of *MAT_036 with m=2, the necessary hardening curve is much closer to the one identified for *MAT_036 with m=8 because the effect of the R-value also contributes for the thinning of the specimen.

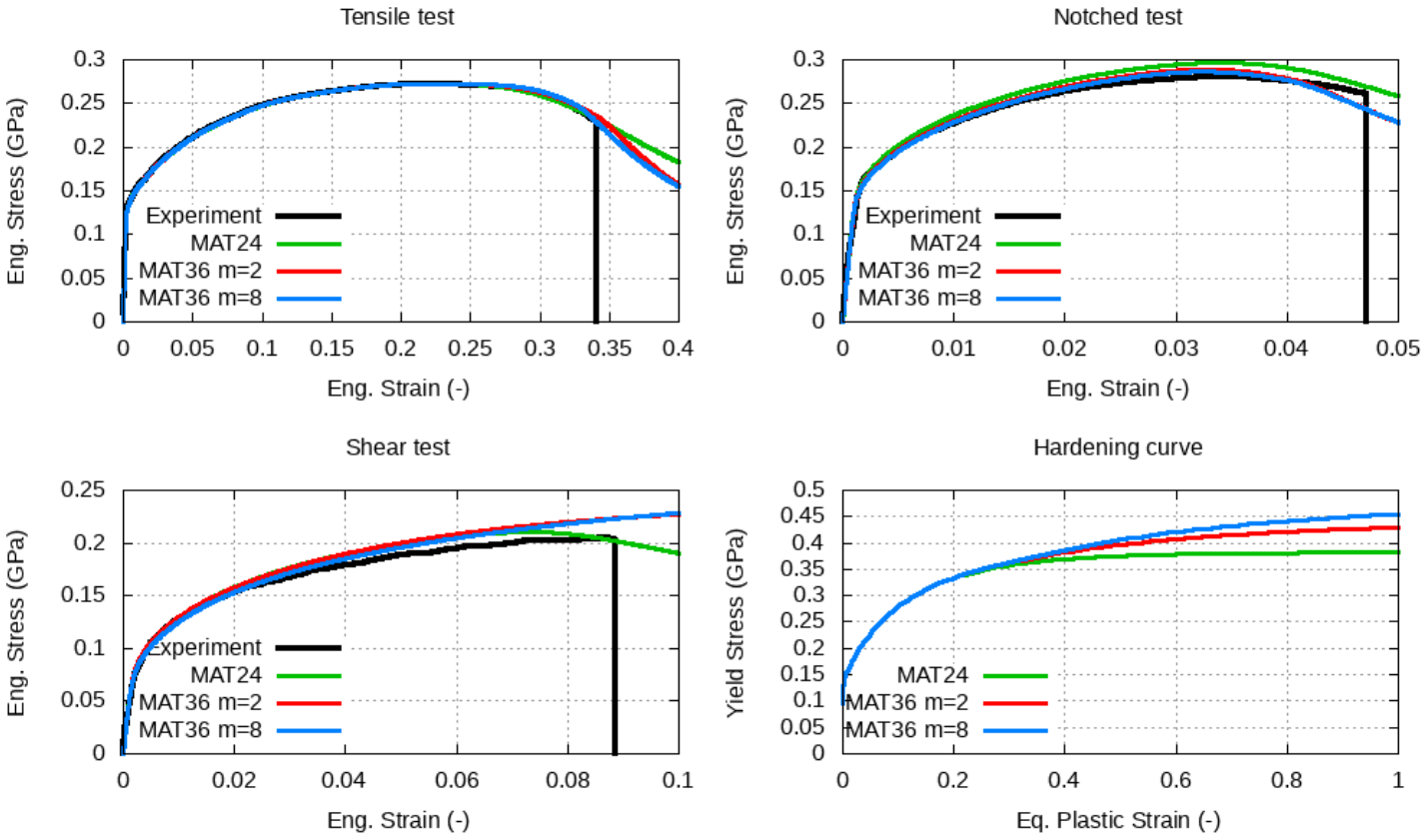

Figure 5. Overview of the simulation results with the different hardening curves.

Looking at the results of the tensile test in Figure 5, one might wonder if all cases could effectively reproduce the material behavior observed in the physical test as the match of the engineering stress strain curve is actually quite accurate. However, in order to verify if the experiment is being correctly reproduced, the strain fields have also to be considered (see Figures 6 and 7). As can be seen from those figures, the contours of major strain can be reproduced almost equally well for all cases. A significant difference is only seen when the minor strain is considered in the analysis. In this case, the solution with *MAT_024 is clearly the one which gives the worst agreement with the experimental data. On the other hand, the differences between *MAT_036 with m=2 and m=8 are marginal for the present material modeling.

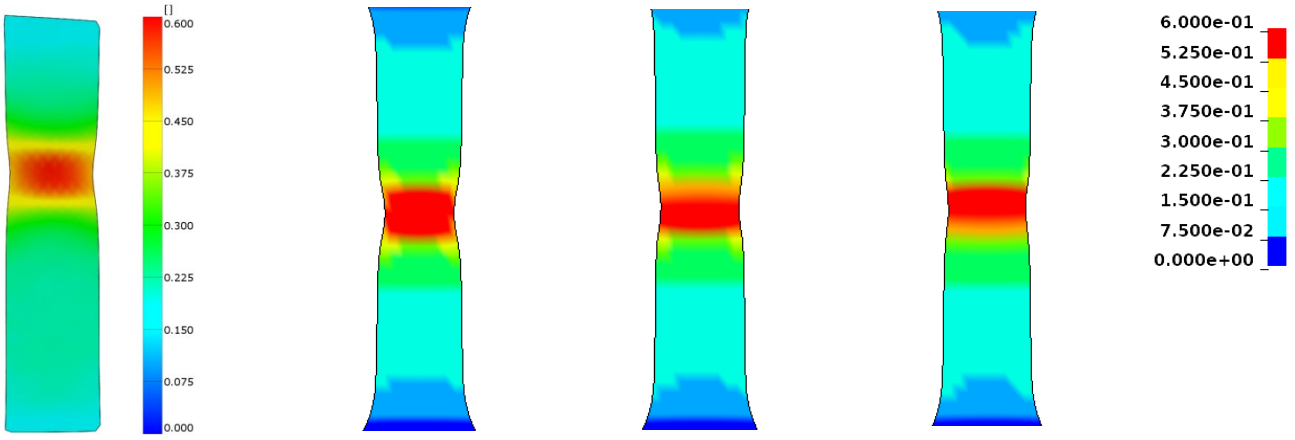

(a) Experiment (b) *MAT_024 (c) *MAT_36 m=2 (d) *MAT_36 m=8

Figure 6. Contours of major strain. Different hardening curves were used in the simulations in (b), (c) and (d) in order to achieve the best agreement with experiments.

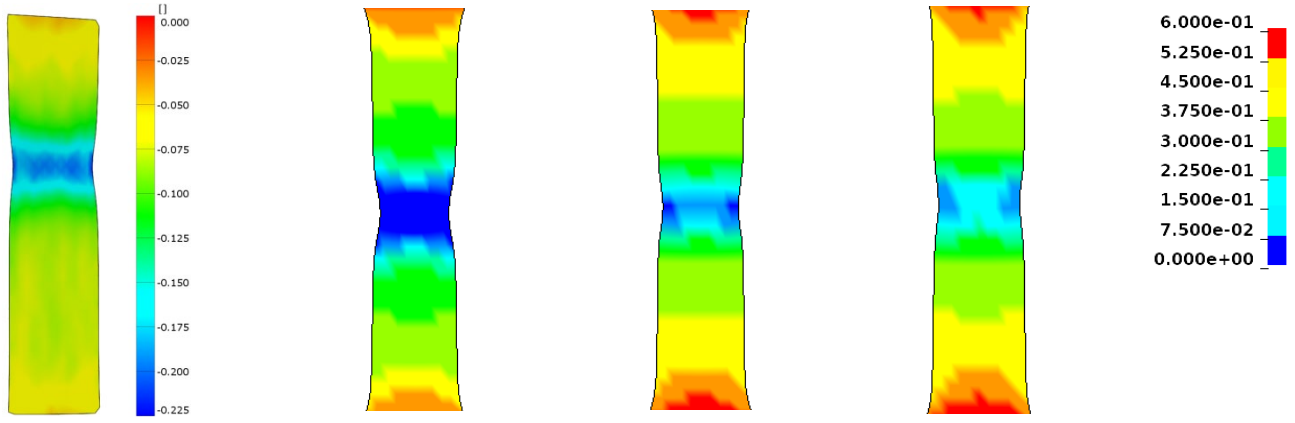

(a) Experiment (b) *MAT_024 (c) *MAT_36 m=2 (d) *MAT_36 m=8

Figure 7. Contours of minor strain. Different hardening curves were used in the simulations in (b), (c) and (d) in order to achieve the best agreement with experiments.

The present analysis also shows the influence of the choice of the material model for the description of the material behavior. Some users tend to think that the hardening curve is an intrinsic property of the material. However, this does not make much sense without mentioning the adopted material formulation (i.e., the material model). As a matter of fact, the different formulations consider different effects stemming from the observed material behavior in physical tests. For instance, *MAT_024, a von Mises based material model, does not consider the effect of the ratio between the second and the third principal strains (i.e., the R-value). However, this effect can be directly measured from experiments and very often it does not agree with the predictions made by *MAT_024. If one aims to use this material model for the best possible description of his material, one basically has to identify the best possible hardening curve in order to reproduce the experimental data, which is what was undertaken in Figure 5. However, because no R-value was considered at all, one can see that the second principal strain could not be correctly predicted, no matter how much the hardening curve was adjusted. Furthermore, the identified hardening curve is considerably flatter than the ones obtained for *MAT_036. In the present case, it was still possible to find such a solution. However, very often the limit of the flatness[1] of the hardening curve for *MAT_024 is quickly achieved and one still does not have a good agreement with the experiment. In such cases, basically, the only possible way to achieve a better agreement with the physical test is by using a material model which can describe the physical phenomenon behind the material deformation in a more accurate manner. For the present alloy, *MAT_036 seems to suffice for that goal.

For completion, the parameters for the GISSMO damage/failure model are identified for the case *MAT_036 with m=2 (see Figure 8). In the present parameter identification procedure, the damage exponent was identified as DMGEXP=2 and the fading exponent as FADEXP=4.0 (see *MAT_ADD_DAMAGE_GISSMO in [2]).

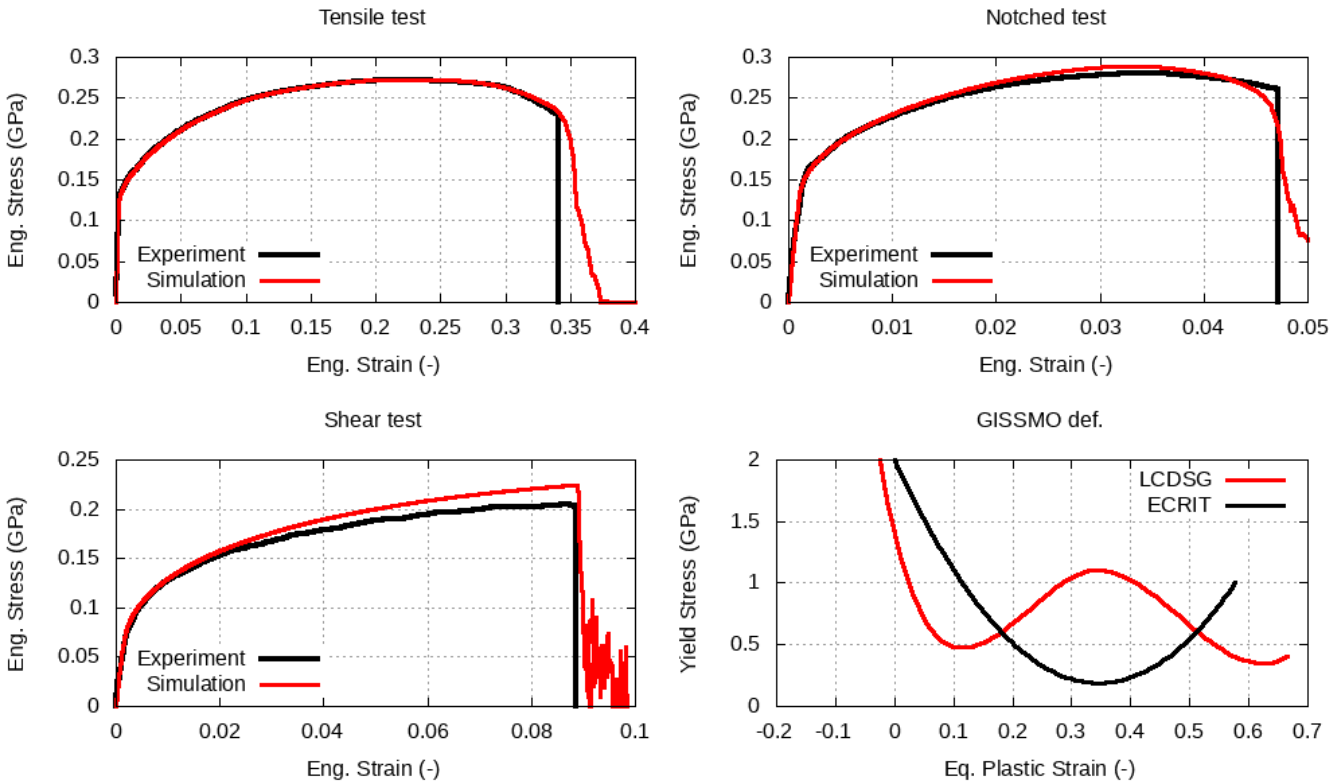

Figure 8. Final calibration of *MAT_036 (m=2, R00=R45=R90=0.6) and GISSMO (*MAT_ADD_DAMAGE_GISSMO).

[1] In fact, the limit of flatness is $\partial\sigma_y/\partial\varepsilon_p = H = 0$ for two reasons: analytic functions for the extrapolation (like Voce or Hocket-Sherby) generally cannot describe softening and setting H<0 means imposing material instability (which should be generally avoided).

Performance Study

The performance of *MAT_036 compared to the one observed by the modelling with *MAT_024 is analyzed in this Section. In this respect, it is important to know if the use of the anisotropic model leads to a significant increase in computational time.

It is however important to emphasize that performance studies of material models can be somewhat challenging. In a typical simulation, many aspects may influence the efficiency of the calculation, like the contact algorithm, the communication between processors in case of parallel processing, among others. Therefore, any performance study of a material model should concentrate on the material model itself as much as possible by reducing the influence of the other aspects. For instance, in order to avoid the influence of the communication between processors, it is important to undertake all simulations using only one and always the same processor.

In the present study, we simulate two cases: (a) a typical tensile test and (b) a typical prismatic profile. We should emphasize that the profile used here serves merely as a numerical example for the purpose of scrutinizing the performance of the material models. This exact profile geometry has not been physically tested for the material studied in this paper.

The main condition for the performance test is that it has been run only on a single and always on the same processor for all cases. For each geometry (i.e., the tensile test and the profile), three runs have been undertaken: one with the *MAT_024 and two with the *MAT_036 material card with exponents m=2 and m=8. No failure through *MAT_ADD_DAMAGE_GISSMO was considered in order to avoid any influence on performance through the damage/failure model. The goal is to determine if *MAT_036 takes longer to compute than *MAT_024 (which is presumable) and, if this is true, what is the increase in computational time. Figures 9 and 10 show the tensile test and the profile at their final configuration for *MAT_024 (top) and *MAT_036 with m=2 (bottom).

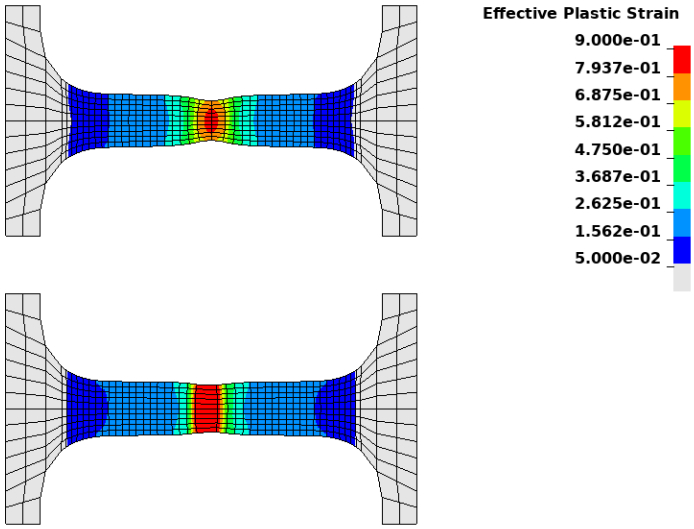

Figure 9. Final configuration of the tensile test for *MAT_024 (top) and *MAT_036 with m=2 and R00=R45=R90=0.6 (bottom), simulation without failure (the final configuration here is beyond the failure point observed in the experiment).

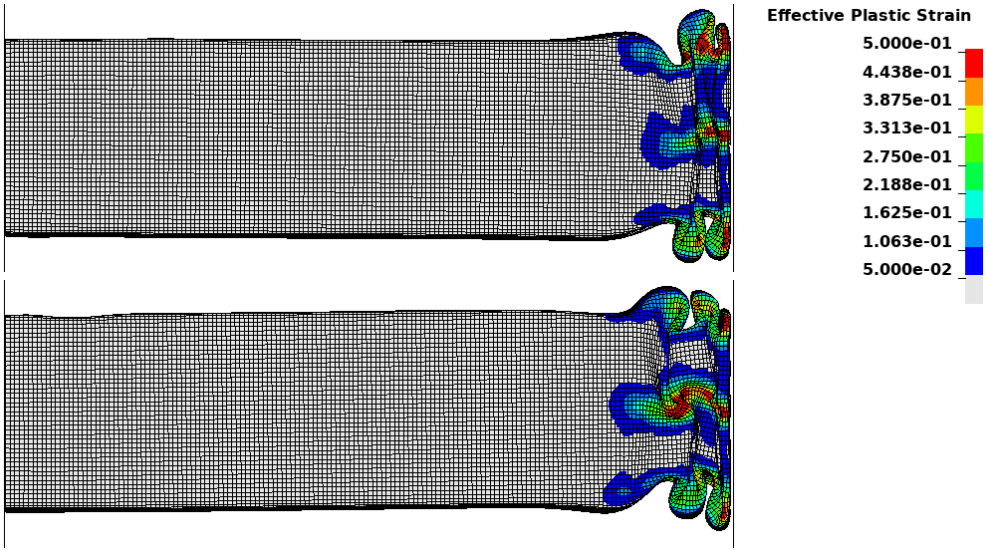

Figure 10. Final configuration of the profile simulation for *MAT_024 (top) and *MAT_036 with m=2 and R00=R45=R90=0.6 (bottom), simulation without failure.

The computer processor used in the present analysis was an Intel® Xeon® E5-2660 v3 with a frequency of 2.60 GHz. The intention behind scrutinizing the numerical efficiency with different exponents in *MAT_036 may, at first glance, sound unimportant, but it does have a justification. Looking at Eq. (3), it is clear that m=2 leads to the calculation of a square root meanwhile m=8 will demand the eighth root of the same operand. Computationally speaking, the calculation of roots which are different than the square root generally takes longer. Therefore, it is quite important to verify if the solution with m=8 is as efficient as the one with m=2.

Tables 1 and 2 show a summary of all performance results obtained in the presented analysis. The information about percentage of element processing, CPU time per zone cycle as well as total time is extracted directly from the d3hsp file from the simulations with LS-DYNA. The left- and right-hand factors are respectively determined by dividing the CPU time per zone cycle and the total time by the ones obtained for *MAT_024 (which was always the most efficient material model). The information about the element processing shows how much simulation time was spent in this task which, in turn, directly involves the material routine. The values above 90% demonstrate that all other factors have been considerably reduced and, therefore, the analysis is suitable for assessing the efficiency of the material models.

For the case when *MAT_036 was run with m=2, an increase of around 30% in computational time could be observed for the tensile test as well as for the profile simulation. However, if we change the exponent to m=8, the computational time increases dramatically. Although not reported in detail in this contribution, a profiling analysis of the different cases was undertaken and this has clearly shown that the increase of computational time is coming from the compiler's internal routine for calculating the eighth root in the yield function.

The increase in computation of time for m=8 in the case of the profile simulation is indeed less pronounced than in the case of the tensile test. This probably is stemming from the fact that the profile has fewer elements under plasticity than the tensile test. In other words, the fewer times the eighth root has to be calculated, the more efficient the material routine.

Table 1. Timing information, tensile test simulation (L_e=0.5mm), double precision

	Element proc.	CPU time per zone cycle	Total time	Factor
***MAT_024**	96%	3178 nanosec	2min53sec	1.0
***MAT_036, m=2**	97%	4428 nanosec	3min49sec	1.39 / 1.32
***MAT_036, m=8**	98%	8009 nanosec	6min33sec	2.52 / 2.27

Table 2. Timing information, profile simulation (L_e=3mm), single precision

	Element proc.	CPU time per zone cycle	Total time	Factor
***MAT_024**	93%	1631 nanosec	1h00min	1.0
***MAT_036, m=2**	95%	2207 nanosec	1h20min	1.35 / 1.33
***MAT_036, m=8**	96%	3043 nanosec	1h56min	1.86 / 1.93

Conclusions

Transversal anisotropy can be considered in crash simulations in a quite straightforward manner because the material directions do not have to be known. The through-thickness anisotropy can then be effectively described through R-values which do not vary in the material plane. In this paper, we investigated the effect of such modeling strategy for an aluminum sheet whose R-values in the different material directions were very similar to each other. It has been shown that the modeling of the transversal anisotropy has indeed described the local strain fields optically measured in experiments more accurately. The additional computation cost involved is reasonable if a quadratic yield function (i.e., m=2 in *MAT_036) is used where a performance study has shown that the anisotropic model needs around 30% longer than *MAT_024. Such increase is quite acceptable for full car crash simulations because not every part in the vehicle is composed of aluminum sheets and therefore the overall additional computational time is actually less than 30%. The solution with m=8, however, does not seem interesting for crash simulations because the increase in computational time is quite considerable and, at least for the present alloy, the benefit in the material description is minimal when compared to the solution with m=2. Therefore, we can conclude that, for the present alloy, a quite interesting modeling solution is the use of *MAT_036 with m=2 and R00=R45=R90=0.6.

Acknowledgements

The authors would like to thank K. Schweizerhof, T. Erhart and A. Haufe for their valuable hints and comments regarding the performance study carried out in this paper.

References

[1] Barlat, F., Lian, J.: “Plastic behavior and stretchability of sheet metals. Part I: A yield function for orthotropic sheets under plane stress conditions”, Int. J. Plasticity 5, 1989, 51-66.

[2] LTSC: “LS-DYNA Keyword User’s Manual – Volume II: Material Models”, Livermore, 2019.